Micro-motion Feature Extraction Based on Bayesian Inference

Le Kang[1,2], **Qun Zhang**[1,2,3], **Ying Luo**[1,2], **Jian Hu**[1,2], **and Yong Wu**[4]

[1]Information and Navigation College, Air Force Engineering University, Xi'an 710011, China
[2]Collaborative Innovation Center of Information Sensing and Understanding, Xi'an 710071, China
[3]Key Laboratory for Information Sensing of Electromagnetic Wave
Fudan University, Shanghai 200433, China
[4]Shaanxi Institute of Metrology, Xi'an 710065, China

Abstract— The micro-Doppler (m-D) effect caused by periodic Doppler modulation of the micro motions such as rotation, vibration, coning motion and precessional motion is widely used in target recognition by estimating the m-D parameters. In this paper, the echo signal of micro-motion targets is projected on the m-D parameter domain to obtain the sparse representation and the m-D parameter estimation can be regarded as the problem of sparse signal recovery. To estimate all three m-D parameters efficiently, a novel parametric Bayesian compressive sensing (BCS) reconstruction algorithm is proposed, in which the Doppler repetition period and Doppler amplitude are discretized to structure an over-complete dictionary and the initial phase estimation is transformed into a dictionary mismatch problem, which is solved by the sparse Bayesian inference. The effectiveness of the proposed method is validated by simulations.

1. INTRODUCTION

Micro-motions such as rotation, vibration, coning motion, or precessional motion, which depends on physical properties like mass distribution characteristics and dynamic characteristics of a target or its parts, may bring additional modulation of the echo signal, which is called m-D effect, except the Doppler modulation caused by translation of target or target component. Micro-motion futures can be extracted via parameters estimation of the modulated echo signal such as initial phase, Doppler amplitude and Doppler repetition period and this technique is called m-D parameter estimation [1]. Currently, future extraction and recognition of micro-motion is considered to be one of the most potential radar target recognition techniques and the micro-Doppler (m-D) effect attracts most attention in the field of academe and industry such as ballistic target recognition, ship identification and human behavior understanding [2, 3].

Since the concept of m-D is proposed [1], time-frequency (t-f) analysis has been widely studied due to the capability to visualize the time varying future of the echo signal and to obtain the characteristics of targets. However, the TF analysis tools have their own defects. Short-time Fourier transform (STFT) could not obtain high t-f resolution simultaneously [1], Wigner-Ville distribution (WVD) may suffer from the cross-term interference for the bilinear transformation and pseudo-Wigner-Ville distribution (PWVD) and reassigned smoothed PWVD (RSPWVD) will lose t-f resolution when echo signal is corrupted by strong noise or only a few measurements are available [4, 5]. Owing to the compressive sensing (CS) theory has successful applications in the fields of satellite communications, navigation, radar, medical imaging, several studies introduce CS into micro-motion signature extraction. Appling CS to characterize the t-f domain, the WVD coefficients are reconstructed from the sparse observation of the ambiguity function [6]. However, the accurate m-D parameter estimation still depends on the Hough transform to map the m-D parameter space onto the t-f domain. To extract the m-D feature for wideband imaging radar [7], complex image orthogonal matching pursuit (OMP) decomposition has been proposed to estimate the m-D parameters directly but computational complexity is not satisfying because five parameters are discretized to build the m-D parameter space. Combining the parametric sparse representation and pruned OMP [8], the m-D parameters are estimated accurately when the Doppler repetition period is considered as constant.

In this paper, considering that both of the Doppler repetition and period Doppler amplitude are not the same for all scatterers on the group targets while the initial phase vary for different scatterers can be regarded as the independent random variable of uniform distribution, the over-complete dictionary is built by discretized Doppler repetition period and Doppler amplitude with the mismatch problem [9] caused by the unknown vector of initial phase. Then the accurate m-D parameter estimation are obtained via sparse Bayesian inference. The group targets micro-motion futures are extracted via separation of multi-component sinusoidal frequency modulation signals [10]

and estimation of the m-D parameters including the initial phase, the Doppler amplitude and the Doppler repetition period. The rest of this paper is organized as follows. The micro-Doppler signal model and CS is reviewed in Section 2. The gridless CS model of micro-Doppler signals is formulated and the solution based on Bayesian inference is proposed for the estimation of micro-Doppler parameters in Section 3. In Section 4, the proposed approach is validated by simulation results. In Section 5, concluding remarks are provided.

2. MICRO-DOPPLER SIGNALS MODELS

The geometrical model between radar and three-dimensional rotating target is shown in Fig. 1, in which the global coordinate system (W, V, U) is stationary and located at the origin Q, the reference coordinate systems (X, Y, Z) is parallel to the global coordinate system and located at the origin O. As shown in Fig. 1, the target can be modeled as a rigid body with a translation velocity v with respect to the radar. The origin of the target coordinate system (x, y, z) is the same as the reference coordinate system. The angular velocity of target can be represented in the target coordinate system as $\boldsymbol{\omega} = (\omega_x, \omega_y, \omega_z)^T$ or represented in the reference coordinate system as $\hat{\boldsymbol{\omega}} = (\omega_X, \omega_Y, \omega_Z)^T$ in the reference coordinate system, where ω_{axis}, axis $= x, y, z, X, Y, Z$ denotes the angular velocity rotating round the corresponding axis. At the initial time, the coordinate of scatterer P_i on the k-th target is $r_0 = (r_{x0}, r_{y0}, r_{z0})^T$ in the target coordinate system and $\widehat{r}_0 = (r_{X0}, r_{Y0}, r_{Z0})^T$ in the reference coordinate system. The transformation between the target coordinate systems and the reference coordinate systems depends on the Euler rotation matrix $\mathbf{R}_{\text{init}}$ [1]. The range vector from the radar to the scatterer is

$$r(t) = \left|\overrightarrow{QP'}\right| = \left|\overrightarrow{QO} + \overrightarrow{OO'} + \overrightarrow{O'P'}\right| = \left\|R_0 + vt + \mathbf{R}_{\text{rotating}}\widehat{r}_0\right\| \tag{1}$$

where $\mathbf{R}_{\text{rotating}}$ denotes the rotation matrix and $\|\cdot\|$ represents the Euclidean norm.

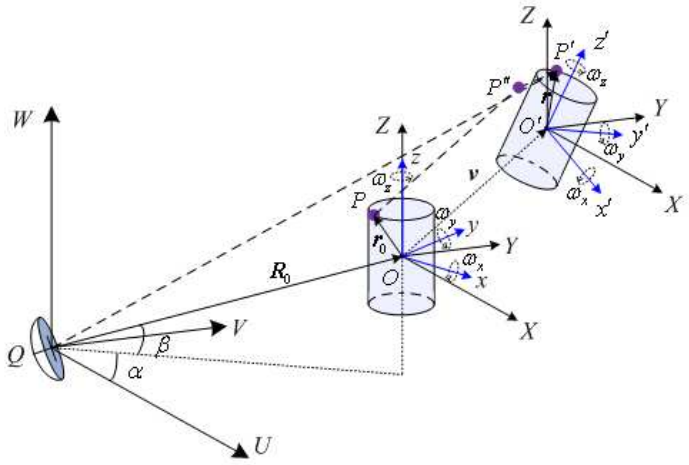

Figure 1: Geometrical relationship between radar and the three-dimensional rotating target.

Supposed that the radar transmits a single frequency continuous-wave with a carrier frequency f_c, the echo signal after baseband transformation can be expressed as

$$s_b(t) = \sigma \exp\left(j2\pi f_c \frac{2r(t)}{c}\right) = \sigma \exp\left(j\Phi(t)\right) \tag{2}$$

where σ is the reflectivity coefficient of the point scatterer, $\Phi_{ki}(t) = j4\pi f_c r(t)/c$ is the phase of the baseband signal and $r(t)$ is the scatterer position. By taking the time derivative of the phase, the Doppler frequency shift of the echo signal [9] and can be written as

$$f_d = \frac{1}{2\pi}\frac{d\Phi(t)}{dt} = \frac{2f_c}{c}\left[v + \frac{d}{dt}\left(\mathbf{R}_{\text{rotating}}\widehat{r}_0\right)\right]^T n \tag{3}$$

where n is the unit vector of $|\overrightarrow{QP'}|$. The m-D frequency is the second term in (4) can be further expressed as

$$f_{\text{m-D}} = \frac{2f_c\Omega}{c}\left\{\left[\hat{\boldsymbol{\omega}}'^2\sin(\Omega t) + \hat{\boldsymbol{\omega}}'\cos(\Omega t)\right]\mathbf{R}_{\text{init}}r_0\right\}^T n \tag{4}$$

which is a time-varying sinusoidal signal whose amplitude is determined by the carrier frequency, the angular velocity, the initial vector and the direction of radar sight line; frequency is the angular rotation frequency Ω.

Although the above mentioned analysis is an example based on a rotating target, which is very common in mechanical and control systems, the m-D signals corresponding to other kinds of micro-motion inducing vibration, coning motion can be abstracted as multi-component sinusoidal frequency modulation signals [10–12], which can be expressed as

$$y(t) = \sum_{k=1}^{K} a_k \exp\left\{j\frac{4\pi}{\lambda}d_k\sin(w_k t + \theta_k)\right\}, \quad t = t_1, t_2, ..., t_M \tag{5}$$

where K is the number of the scatterers, a_k denotes the complex reflectivity of the kth scatterer, d_k is related to the position if the kth scatterer and varies directly as the maximal Doppler amplitude, λ is the wavelength, θ_k is the initial phase and dependent on the geometrical relationship between the kth scatterer and the rotation center, and w_k is the angular velocity of the kth scatterer. By taking the time derivative of the phase term in (6), them-D frequency of the kth scatterer can be written as

$$f_{\text{m-D}} = \frac{2}{\lambda}d_k w_k \sin(w_k t + \theta_k) \tag{6}$$

The m-D parameters which need to be estimated is $\{d_k, w_k, \theta_k\}$ for $k = 1, 2, ..., K$. Considering w_k as a constant for single target, the m-D parameter estimation can be transformed to parametric sparse representation model, which is not applicable in the case of group targets.

3. THE PROPOSED APPROACH

3.1. Gridless CS Model for Micro-Doppler Signals

Considering the set $\mathbf{S} = \{\mathbf{W} \times \mathbf{D}\}$ as the atomic set of the signal in (6), where $\times$ denotes the Cartesian product, $\mathbf{W} = \{w_1, ..., w_p, ..., w_P\}$ and $\mathbf{D} = \{d_1, ..., d_q, ..., d_Q\}$ respectively denote the uniformly discretized angular velocity space that w_k belongs to and the Doppler amplitude space that d_k belongs to, the signal in (6) can be expressed as

$$\mathbf{Y} = \mathbf{A}(\boldsymbol{\theta}) \cdot \mathbf{X} + \mathbf{E} \tag{7}$$

where $\mathbf{Y} = [y(t_1), y(t_2), ..., y(t_M)]^T \in \mathrm{C}^{M\times 1}$ and $\mathbf{E} = [e(t_1), e(t_2), ..., e(t_M)]^T \in \mathrm{C}^{M\times 1}$ are the measurement and noise respectively, $\mathbf{X} \in \mathrm{C}^{(PQ)\times 1}$ and PQ typically satisfies $PQ \gg M \gg K$, $\mathbf{A}(\boldsymbol{\theta}) \in C^{M\times(PQ)}$ and the element is

$$\mathbf{A}(\boldsymbol{\theta})_{m,p+(q-1)P} = \exp\left\{j\frac{4\pi}{\lambda}d_q\sin(w_p t_m) + \theta_{p+(q-1)P}\right\} \tag{8}$$

$\mathbf{X}_{p+(q-1)P} = a_k$ if and only if $\mathbf{S}_{p+(q-1)P} = (d_k, w_k)$, otherwise $\mathbf{X}_{p+(q-1)P} = 0$. The above mentioned model, which is called on-grid CS model, is based on the projection of the initial phase on the uniformly discretized grids. However, the off-grid parameter may cause larger error and miss the most sparse solution of $\mathbf{X}$, which is called mismatch problem [13]. Supposed $\hat{\boldsymbol{\theta}} = \{\hat{\theta}_1, \hat{\theta}_2, ..., \hat{\theta}_{PQ}\}$ is a fixed sampling set and each element belongs to $[0, 2\pi]$. Of course, the real initial phase $\theta_k \notin \{\hat{\theta}_1, \hat{\theta}_2, ..., \hat{\theta}_{PQ}\}$ from some $k \in \{1, 2, ..., K\}$ and $\hat{\theta}_{nk}, n_k \in \{1, 2, ..., PQ\}$ is the nearest value to θ_k. Using linearization to approximate the column of $\mathbf{A}$:

$$\mathbf{a}(\theta_k) \approx \mathbf{a}\left(\hat{\theta}_{nk}\right) + \boldsymbol{\Delta}\left(\hat{\theta}_{nk}\right)\left(\theta_k - \hat{\theta}_{nk}\right) \tag{9}$$

where $\Delta(\hat{\theta}_{nk}) = \mathbf{a}'(\hat{\theta}_{nk})$. Denote $\mathbf{A} = [\mathbf{a}(\hat{\theta}_1), \mathbf{a}(\hat{\theta}_2), ..., \mathbf{a}(\hat{\theta}_{PQ})]$, $\mathbf{B} = [\boldsymbol{\Delta}(\hat{\theta}_1), \boldsymbol{\Delta}(\hat{\theta}_2), ..., \boldsymbol{\Delta}(\hat{\theta}_{PQ})]$, $\beta = [\beta_1, ..., \beta_{PQ}]^T \in [-\pi, \pi]^N$ and $\boldsymbol{\Phi}(\beta) = \mathbf{A} + \mathbf{B}\mathrm{diag}(\beta)$, where for $n = 1, 2, ..., PQ$,

$$\begin{aligned} &\beta_n = \theta_k - \hat{\theta}_{nk},\ \mathbf{X}_n = a_{nk}, \quad \text{if } n = n_k \text{ for any } k \in \{1, 2..., K\};\\ &\beta_n = 0,\ \mathbf{X}_n = 0, \quad \text{otherwise.} \end{aligned} \tag{10}$$

After merging the approximation error into the observation noise, the signal model in (8) can be further written as

$$\mathbf{Y} = \mathbf{\Phi}(\beta) \cdot \mathbf{X} + \mathbf{E} \tag{11}$$

In fact, the gridless CS model in (12) can be regarded as the first order approximation of the real measurement model while the one without initial phase is the zeroth order approximation. As a result, the gridless CS model can estimated the initial phase to find the most sparse solution of $\mathbf{X}$ with two advantages than the on-grid CS model. One is that the gridless model has higher accuracy, particularly in the low noise environment where the modeling error takes the main part rather than the uncertainly error. The other is that looser grids can be applied in the gridless model to reduce computational cost with a comparable accuracy.

3.2. The Bayesian Inference

To estimate m-D parameters including Doppler repetition period, Doppler amplitude and initial phase based on CS, we should make the most of the sparse prior information of the targets. The methods to unitized the prior information mainly include deterministic model and Bayesian model. In fact, a deterministic model can transforms into a Bayesian model by appropriate probability density functions (PDF) [14], the estimates for $\mathbf{X}$ and β can be cast as the MAP estimation.

In this paper, a bilayer hierarchical prior model is employed [14, 15], which is widely used in Bayesian inference, to get the sparse prior information on $\mathbf{X}$. Define that

$$p\left(\mathbf{X}\left|\Upsilon\right.\right) = CN\left(\mathbf{X}\left|0,\mathbf{V}\right.\right) = \prod_{i=1}^{PQ} \frac{1}{(2\pi\gamma_i)} \exp\left\{-\frac{|x_i|^2}{2\gamma_i}\right\} \tag{12}$$

$$p\left(\Upsilon\left|a,b\right.\right) = \prod_{i=1}^{PQ} \Gamma\left(\gamma_i\left|a,b\right.\right) = \prod_{i=1}^{PQ} \frac{b^a \gamma_i^{a-1}}{\Gamma\left(a\right)} \exp\left(-b\gamma_i\right) \tag{13}$$

where $\mathbf{V} = \mathrm{diag}(\Upsilon)$, $\Upsilon = [\gamma_1, \gamma_2, ..., \gamma_{PQ}]$ is the hyper-parameter of the complex Gaussian distribution, $\Gamma(\cdot)$ denotes the Gamma function, $a > 0$ and $b > 0$.

The PDF of the white Gaussian noise with unknown variance σ^2 the can be expressed as

$$p\left(\mathbf{E}\left|\sigma^2\right.\right) = CN\left(\mathbf{E}\left|0,\sigma^2\mathbf{I}\right.\right) = \frac{1}{\pi^{PQ}\left|\sigma^2\mathbf{I}\right|} \exp\left\{-\left(\mathbf{E}-0\right)^H \sigma^{-2}\mathbf{I}\left(\mathbf{E}-0\right)\right\} \tag{14}$$

Then the likelihood function of $\mathbf{Y}$ can be written as

$$p\left(\mathbf{Y}\left|\mathbf{X},\sigma^2,\beta\right.\right) = CN\left(\mathbf{Y}\left|\mathbf{\Phi}(\beta)\cdot\mathbf{X},\sigma^2\mathbf{I}\right.\right) = \left(\frac{1}{2\pi\sigma^{-2}}\right)^{PQ} \exp\left\{-\frac{1}{2\sigma^2}\left\|\mathbf{Y}-\mathbf{\Phi}(\beta)\mathbf{X}\right\|^2\right\} \tag{15}$$

Considering Gamma distribution and Gaussian distribution are conjugated with each other, the gamma prior is assumed for the unknown variance of noise as follow

$$p\left(\sigma^{-2};c,d\right) = \Gamma\left(\sigma^{-2}\left|c,d\right.\right) \tag{16}$$

where c and d are set to approach zero to obtain a broad hyperprior of the variance [15]. Based on the conjugate property and the Bayesian principle, the joint PDF can be written as

$$p\left(\mathbf{X},\mathbf{Y},\beta,\sigma^2,\Upsilon\right) = p\left(\mathbf{Y}\left|\mathbf{X},\beta,\sigma^2\right.\right) p\left(\mathbf{X}\left|\Upsilon\right.\right) p\left(\Upsilon\left|a,b\right.\right) p\left(\sigma^2\right) p(\beta) \tag{17}$$

where the PDF on the right side is defined as (16), (13), (14), broad hyperprior of (17) respectively and the β obeys the uniform distribution as

$$\beta \sim U\left(\left[-\pi,\pi\right]^{PQ}\right) \tag{18}$$

The off-grid distance β is assumed to obey uniformly distributed rather than Gaussian distributed in [16] because that the off-grid distance is related to the initial phase, which can be considered as an uninformative variable except the boundary. Then the posterior distribution of $\mathbf{X}$ obeys

$$p\left(\mathbf{X}\left|\mathbf{Y},\beta,\sigma^2,\Upsilon\right.\right) = CN\left(\mathbf{X}\left|\mu,\sum\right.\right), \quad \mu = \sigma^{-2}\sum \mathbf{\Phi}^H\mathbf{Y}, \quad \sum = \left(\sigma^{-2}\mathbf{\Phi}^H\mathbf{\Phi} + \mathbf{V}^{-1}\right)^{-1} \tag{19}$$

To obtain the mean μ and the variance $\sum$, the β, σ^2 and Υ are estimated by the MAP estimation method to maximize $p(\beta, \sigma^2, \Upsilon \,|\mathbf{Y})$, which is proportional to the joint PDF $p(\mathbf{Y}, \beta, \sigma^2, \Upsilon) = p(\beta, \sigma^2, \Upsilon \,|\mathbf{Y})p(\mathbf{Y})$ because $p(\mathbf{Y})$ is irrelevant to the β, σ^2 and Υ. Integrating (18) with respect to $\mathbf{X}$ to obtain $p(\mathbf{Y}, \beta, \sigma^2, \Upsilon)$ and uilizing the expectation-maximization (EM) algorithm, the updates of σ^2 and Υ are can be written as [15]

$$\sigma^2 = \frac{PQ + c - 1}{E\left\{\|\mathbf{Y} - \mathbf{\Phi}(\beta)\mathbf{X}\|^2\right\} + d}, \quad \gamma_i = \frac{\sqrt{1 + 4bE\left\{\|\mathbf{X}_i\|^2\right\}} - 1}{2b}, \quad i = 1, 2, ..., PQ \tag{20}$$

where $E\{\|\mathbf{X}_i\|^2\} = \|\mu_i\|^2 + \sum_{ii}$ and $E\{\|\mathbf{Y} - \mathbf{\Phi}(\beta)\mathbf{X}\|^2\} = \|\mathbf{Y} - \mathbf{\Phi}(\beta)\mu\|^2 + \sigma^2 \sum_{i=1}^{PQ}(1 - \sigma^2 \sum_{ii})$. As for β, we can obtain by maximizing $E\{p(\mathbf{Y} \,|\mathbf{X}, \beta, \sigma^2)p(\beta)\}$ and derive as

$$\begin{aligned}
\max_{\beta} E\left\{p\left(Y \,|X, \beta, \sigma^2\right) p(\beta)\right\} &= \min_{\beta} E\left\{\|Y - (A + B\mathrm{diag}\,(\beta))\, X\|^2\right\} \\
&= \min_{\beta}\Big\{ \|Y - (A + B\mathrm{diag}(\beta))\,\mu\|^2 \\
&\quad + \mathrm{Tr}\left\{(A + B\mathrm{diag}(\beta)) \sum (A + B\mathrm{diag}(\beta))^H\right\}\Big\} \\
&= \min_{\beta}\left(\beta^T G\beta - 2J^T\beta + C\right)
\end{aligned} \tag{21}$$

where $G = \Re\{(B^H B) \odot (\mu\mu^H + \sum)\}$ and $J = \Re\{\mathrm{diag}(\mu)B^H(Y - A\mu)\} - \Re\{\mathrm{diag}(B^H A \sum)\}$. To obtain an explicit expression from (22), $\hat{\beta} = G^{-1}J$ by setting $\frac{\partial}{\partial\beta}\{\beta^T G\beta - 2J^T\beta\}$ to be zero and we can update β by each element by fixing up others as $\hat{\beta}_i = (J_i - (G_i)_{-i}^T \beta_{-i})/G_{ii}$, where $(g)_{-i}$ denotes the origin vector without the ith element or the origin matrix without the ith column. Then the updates of β can be written as

$$\beta_i^{\text{new}} = \begin{cases} \hat{\beta}_i, & \text{if } \hat{\beta}_i \in [-\pi, \pi]\,; \\ -\pi, & \text{if } \hat{\beta}_i < -\pi; \\ \pi, & \text{if } \hat{\beta}_i > \pi. \end{cases} \tag{22}$$

The proposed algorithm can be implemented as follows. Firstly, initialize the parameters β, σ^2 and Υ. Secondly, calculate μ and the $\sum$ based on the last value according to (20) and update σ^2, Υ and β according to (21) and (23). Finally, repeat the second step until the convergence criterion, which is chosen as the same as the EM algorithm [17], is satisfied.

4. SIMULATION RESULTS

To validate the proposed approach, some simulation experiments and performance results are given in this section. We set the carrier frequency is 37.5 GHz, the pulse repetition frequency is 200 Hz and the sampling number is 200. Assume that the three scatterers are respectively set on three targets and the echo m-D signal has three components with parameters $\{\omega_1, \omega_2, \omega_3\} = \{3\pi, 4\pi, 5\pi\}$ rad/s, $\{d_1, d_2, d_3\} = \{4.24, 8.91, 6.24\}$ mm, $\{\theta_1, \theta_2, \theta_3\} = \{0.28\pi, 1.48\pi, 0.5\pi\}$ and $\{a_1, a_2, a_3\} = \{1, 0.9, 0.8\}$. Then the $\{d, \omega\}$ space is discretized into 50×50 grids.

Figures 2–5 are based on noiseless case. Fig. 2 shows the time-frequency plane of the m-D signal obtained by RSPWVD and PWVD. In Fig. 2(a), the three m-D components can be roughly seen but the resolution is very low. In Fig. 2(b), the three m-D components are confused because the cross-term interference is quite serious.

In the proposed approach, the time-frequency analysis is needless, the projection of the echo m-D signal on the $\{d, \omega\}$ space is shown in Fig. 3 and the three m-D components are completely separated. Fig. 4 shows the iteration of the initial phase of the three m-D components and the correct convergent results are obtained after 12 iterations. Then, the reconstructed m-D signal by the estimation of the proposed approach is shown in Fig. 5.

Considering the anti-noise performance and the accuracy of m-D parameter estimation, the proposed approach, Hough-PWVD and Hough-RSPWVD are compared in noisy environments.

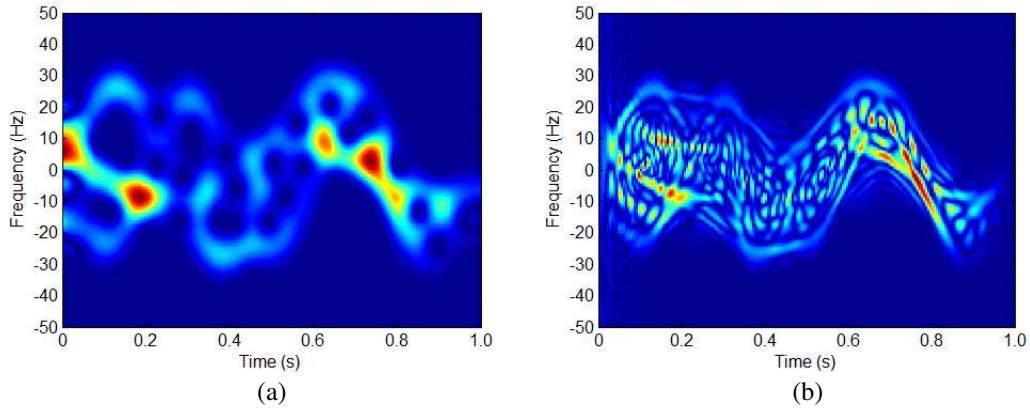

Figure 2: Time-frequency plane of the micro-Doppler signal. (a) RSPWVD. (b) WVD.

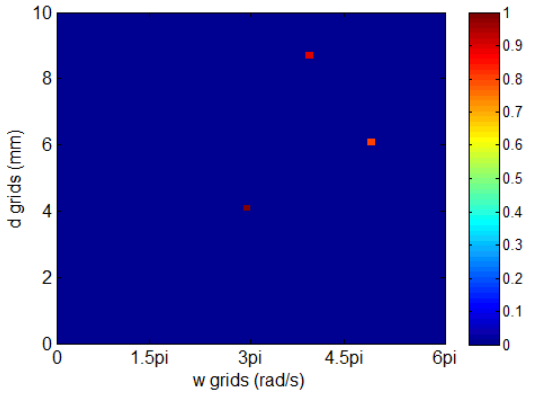

Figure 3: Parameter space of the micro-Doppler signal.

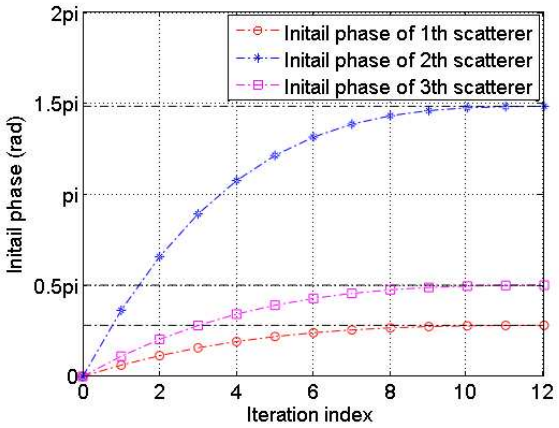

Figure 4: Iteration of the initial phase.

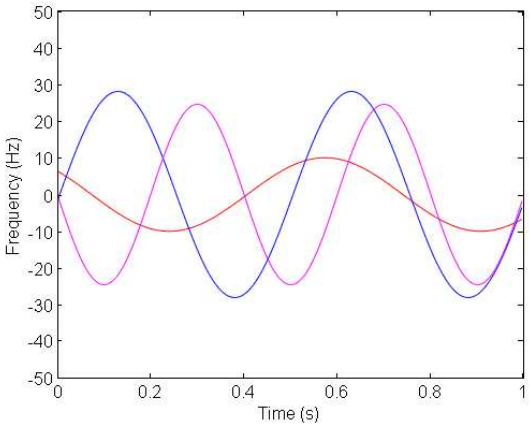

Figure 5: Time-frequency plane of the proposed approach.

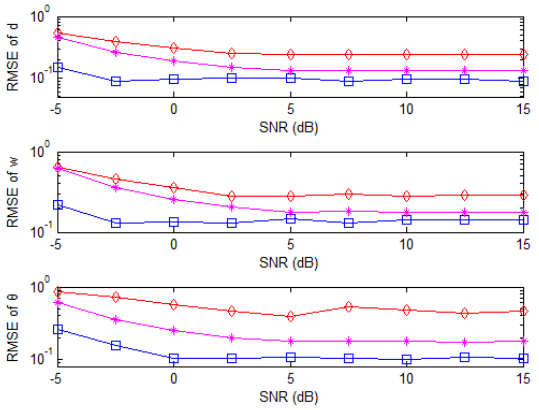

Figure 6: RMSE versus SNR. Diamond, star and square respectively denote the Hough-PWVD, Hough-RSPWVD and proposed algorithms.

The m-D signal is set to composed of three components with different angular velocity to simulate the case of group targets and the m-D parameters are set randomly in the ranges $0 < d_i < 10\,\text{mm}$,

$0 < \omega_i < 6\pi$ rad/s and $0 \leq \theta_i \leq 2\pi$, $i = 1, 2, 3$. The noise is set to additive Gaussian noise and the signal-to noise ratio (SNR) is SNR $= \|Y\|^2/(M\sigma^2)$. The root-mean-squared error (RMSE) versus SNR of the m-D parameter estimation is shown in Fig. 6, in which we can see that the estimation accuracy of the proposed approach is better than the Hough-PWVD and the Hough-RSPWVD algorithms. The number of Monte-carlo trials is 100.

5. CONCLUSION

A novel approach for m-D parameter estimation based on sparse Bayesian learning was proposed. We adopt the gridless CS theory to describe the m-D signal model, which are solved by the Bayesian inference of a two-stage hierarchical prior structure. Compared to the traditional method, the proposed approach can obtain accurate m-D parameter estimation for group targets. Due to the large computation of the Bayesian-based algorithms, how to design fast algorithms is worth investigating in the future.

ACKNOWLEDGMENT

This work was supported by the National Natural Science Foundation of China under Nos. 61571457 and 614.

REFERENCES

1. Chen, V. C., F. Li, S. S. Ho, and H. Wechsler, "Micro-Doppler effect in radar: Phenomenon, model, and simulation study," *IEEE Trans. Aerosp. Electron. Syst.*, Vol. 42, No. 1, 2–21, 2006.
2. Zhang, Q., Y. Luo, and J. He, "Review of researches on micro-Doppler effect of radar targets," *Journal of Air Force Engineering University*, Vol. 12, No. 2, 22–26, 2011.
3. Clemente, C., A. Balleri, K. Woodbridge, and J. Soraghan, "Developments in target micro-Doppler signatures analysis: Radar imaging, ultrasound and through-the-wall radar," *EURASIP J. Adv. Signal Process.*, Vol. 47, No. 1, 1–18, 2013.
4. Chen, V. C., *The Micro-Doppler Effect in Radar*, Artech House, Norwood, MA, USA, 2011.
5. Cirillo, L., A. Zoubir, and M. Amin, "Parameter estimation for locally linear FM signals using a time-frequency hough transform," *IEEE Trans. Signal Process.*, Vol. 56, No. 9, 4162–4175, 2008.
6. Orović, I., S. Stanković, and M. Amin, "Compressive sensing for sparse time-frequency representation of nonstationary signals in the presence of impulsive noise," *Proc. SPIE*, Vol. 8717, May 31, 2013.
7. Luo, Y., Q. Zhang, C. Qiu, S. Li, and T.-S. Yeo, "Micro-Doppler feature extraction for wideband imaging radar based on complex image orthogonal matching pursuit decomposition," *IET Radar Sonar Navig.*, Vol. 7, No. 8, 914–924, 2013.
8. Li, G. and P. K. Varshney, "Micro-Doppler parameter estimation via parametric sparse representation and pruned orthogonal matching pursuit," *IEEE Journal of Selected Topics in Applied Earth Observations and Remote Sensing*, Vol. 7, No. 12, 4937–4948, 2014.
9. Zhang, Q. and Y. Luo, *Mico-Doppler Effect of Radar Targets*, 3–24, National Defend Industry Press, Beijing, 2013.
10. Lei, P., J. Sun, J. Wang, and W. Hong, "Micromotion parameter estimation of free rigid targets based on radar micro-Doppler," *IEEE Trans. Geosci. Remote Sens.*, Vol. 50, No. 10, 3776–3786, 2012.
11. Smith, G. E., K. Woodbridge, C. J. Baker, and H. Griffiths, "Multistaticmicro-Doppler radar signatures of personnel targets," *IET Signal Process.*, Vol. 4, No. 3, 224–233, 2010.
12. Thayaparan, T., L. J. Stankovic, M. Dakovic, and V. Popovic, "Micro-Doppler parameter estimation from a fraction of the period," *IET Signal Process*, Vol. 4, No. 3, 201–212, 2010.
13. Tang, G., B. N. Bhaskar, P. Shah, et al., "Compressed sensing off the grid," *IEEE Transactions on Information Theory*, Vol. 59, No. 11, 7465–7490, 2013.
14. Babacan, S., R. Molina, and A. Katsaggelos, "Bayesian compressive sensing using Laplace priors," *IEEE Trans. Image Process.*, Vol. 19, No. 1, 53–63, 2010.
15. Liu, H., J. Bo, H. Liu, and Z. Bao, "Super resolution ISAR imaging based on sparse Bayesian learning," *IEEE Trans. Geosci. Remote Sens.*, Vol. 52, No. 12, 5005–5013, 2014.
16. Zhu, H., G. Leus, and G. Giannakis, "Sparsity-cognizant total least-squares for perturbed compressive sampling," *IEEE Trans. Signal Process.*, Vol. 59, No. 5, 2002–2016, 2011.
17. McLachlan, G. and T. Krishnan, *The EM Algorithm and Extensions*, Wiley, New York, 1997.